IOPscience iopscience.iop.org

Home Search Collections Journals About Contact us My IOPscience

The mechanism of formation and properties of Li-doped p-type ZnO grown by a two-step heat treatment

This article has been downloaded from IOPscience. Please scroll down to see the full text article.

2006 Semicond. Sci. Technol. 21 494

(http://iopscience.iop.org/0268-1242/21/4/013)

View the table of contents for this issue, or go to the journal homepage for more

Download details:
IP Address: 159.226.165.151
The article was downloaded on 07/09/2012 at 08:14

Please note that terms and conditions apply.

INSTITUTE OF PHYSICS PUBLISHING SEMICONDUCTOR SCIENCE AND TECHNOLOGY

Semicond. Sci. Technol. **21** (2006) 494–497 doi:10.1088/0268-1242/21/4/013

# The mechanism of formation and properties of Li-doped p-type ZnO grown by a two-step heat treatment

**X H Wang[1,2], B Yao[1], Z Z Zhang[1], B H Li[1], Z P Wei[1,2], D Z Shen[1], Y M Lu[1] and X W Fan[1]**

[1] Key Laboratory of Excited State Processes, Changchun Institute of Optics, Fine Mechanics and Physics, Chinese Academy of Science, Changchun 130033, People's Republic of China
[2] Graduate School of the Chinese Academy of Sciences, Beijing 100049, People's Republic of China

E-mail: binyao@jlu.edu.cn

Received 18 November 2005, in final form 24 January 2006
Published 2 March 2006
Online at stacks.iop.org/SST/21/494

**Abstract**
Li-doped p-type ZnO was fabricated by heat treatment of Zn–Li alloy film with 2 at% Li on a quartz substrate in $N_2$ flow at 500 °C for 2 h, and then in $O_2$ flow at 700 °C for 1 h. The room-temperature resistivity was measured to be 678.34 Ω cm with a Hall mobility of 1.03 $cm^2\ V^{-1}\ s^{-1}$ and a carrier concentration of $8.934 \times 10^{15}\ cm^{-3}$. Three emission peaks centred at 3.347, 3.302 and 3.234 eV are observed in the photoluminescence spectrum measured at 12 K and are due to neutral acceptor-bound exciton emission, conduction band to acceptor level transition and donor–acceptor pair recombination emission, respectively. The p-type conduction of the Li-doped ZnO may be attributed to the formation of a $Li_{Zn}$–N complex acceptor. The optical level of the acceptor is estimated to be about 137 meV. The mechanism of formation of the Li-doped p-type ZnO is discussed in the present work.

## Introduction

ZnO with a direct wide-band gap (3.37 eV) and a larger exciton binding energy (60 meV) has been increasingly studied for many years due to its excellent physical properties (piezoelectricity, conductivity and optical) and applications in blue and ultraviolet light emitting diodes [1], solar cells and surface acoustic wave devices [2, 3]. However, the realization of p-type ZnO in a reproducible way is rather difficult, because of its self-compensating effect, deep acceptor level and low solubility of acceptor dopants. The optimal choice of acceptor species remains to be determined. Theoretical calculation predicted that group-I elements substituting for Zn are of a shallower acceptor level than group-V elements substituting for O, so group-I elements are considered to be better dopants than group-V elements in terms of acceptor levels. Especially the acceptor level of Li substituting for Zn($Li_{Zn}$), which is 0.09 eV [4], the shallowest value among the energy levels of acceptor dopants reported. However, optically detected magnetic resonance experiments show that Li introduces a deep acceptor state [5, 6]. Experimentally, 30% of the Zn sites can be occupied by Li in single crystal ZnO [7]. However, when Li atoms substitute for Zn, it will easily be accompanied by the formation of interstitial Li($Li_i$), which are likely to be shallow donors [8]. This causes the p-type doping to be limited by the formation of a $Li_{Zn}$–$Li_i$ complex donor. In order to resolve such a problem, we design a new way of preparing Li-doped p-type ZnO by reducing the amount of $Li_i$. The mechanism of formation and properties of the Li-doped p-type ZnO are investigated in the present work.

## Experiment

Quartz was used as a substrate in the present experiment. It was treated with ethanol in an ultrasonic bath to remove surface contamination and etched in HCl solution at 80 °C for 10 min, and then rinsed in deionized water (18.2 MΩ cm) and blown dry using high-purity nitrogen. The films of Zn–Li alloy with 1, 2 and 4 at% Li and pure Zn were produced by thermal evaporation in a vacuum system; the base pressure

 © 2006 IOP Publishing Ltd Printed in the UK 

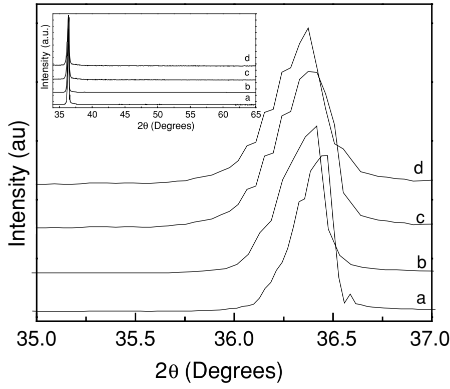


**Figure 1.** XRD patterns of around the (0 0 2) peak of (a) metal Zn and Zn–Li alloy films doped with (b) 1, (c) 2 and (d) 4 at% Li. Inset is the corresponding XRD profile in diffraction angles ($2\theta$) of 34–65°.

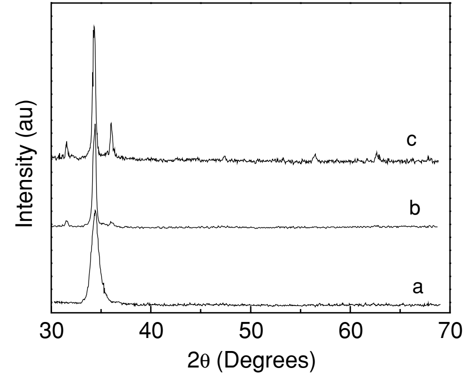


**Figure 2.** XRD patterns of (a) metal Zn, (b) Zn–2 at% Li and (c) Zn–4 at% Li alloy film annealed at 500 °C for 2 h in $N_2$ flow and then at 700 °C for 1 h in $O_2$ flow.

in the vacuum chamber was lower than $5 \times 10^{-5}$ Torr. Each of the films was annealed in two different ways: (1) annealing at 500 °C for 2 h in a $N_2$ flow and then at 700 °C for 1 h in an $O_2$ flow (called annealing in two steps in the following); (2) annealing at 700 °C for 1 h in an $O_2$ flow (called annealing in one step in the following). The metal Zn and Zn–Li alloy films with 1, 2 and 4 at% Li were denoted as samples $A_1$, $B_1$, $C_1$ and $D_1$, respectively, as annealed in two steps and as samples $A_2$, $B_2$, $C_2$ and $D_2$, respectively, when annealed in one step.

The electrical properties of the films were obtained by Hall measurement in the Van der Pauw configuration at room temperature using a current of 300 nA and magnetic fields of 3000–18 000 G (Lakershore HMS 7707). Electrodes were fabricated by depositing metal indium on the surface of films by conventional vacuum evaporation and sintering in vacuum ($\leqslant 10^{-5}$ Torr). Ohmic contact between the indium spots and films was confirmed prior to Hall measurement. The results were averaged in order to compensate for various electromagnetic effects [9]. X-ray diffraction (XRD) measurement was performed by using a Rigaku O/max-RA x-ray diffractometer with Cu K$\alpha$ radiation ($\lambda = 1.5418$ Å). The photoluminescence (PL) of the films was measured at 12 K by a He–Cd laser with 325 nm line.

The inset of figure 1 shows XRD patterns of metal Zn and Zn–Li alloy films with nominal Li content of 1, 2 and 4 at%, respectively. It indicates that all the films were highly preferentially oriented in the (0 0 2) direction. Curves a, b, c and d in figure 1 show XRD profiles of the near (0 0 2) peak of Zn and Zn–Li film with nominal Li content of 1, 2 and 4 at%, respectively, indicating that the *d*-spaces of the (0 0 2) plane of the Zn–Li alloy films are larger than that of the metal Zn film and increase with increasing nominal Li doping content up to about 2 at%. When the nominal Li doping content is above 2 at%, the (0 0 2) *d*-space changes a little. As the metallic radius of Li of 0.152 nm is larger than that of Zn of 0.133 nm, so incorporation of Li into Zn should be in a form of substitute rather than interstitial atom and leads to increase of lattice constants of Zn, that is, increase in the (0 0 2) *d*-space, as shown in figure 1. Due to the limited solubility of Li in metal Zn, the increase of lattice constants with increasing Li content will stop at some Li doping concentration, as seen in figure 1. We estimated solubility of Li ($x$) in the Zn–Li alloy with 1, 2 and 4 at% Li to be about 0.81, 1.63, 1.67 at%, respectively, by using XRD data measured from figure 1 and the modified Vegard formula

$$r_{\text{Zn–Li}} = r_{\text{Zn}} + (r_{\text{Li}} - r_{\text{Zn}})x, \tag{1}$$

where $r_{\text{Zn–Li}}$, $r_{\text{Zn}}$ and $r_{\text{Li}}$ are metallic radii of the Zn–Li alloy, Zn and Li, respectively, and $x$ is the solubility of lithium in a unit of atom per cent. The radius of the Zn or Zn–Li alloy was calculated by a formula of $r = a/2 = (c/1.8563)/2$, where $a$ and $c$ are the lattice constants of the Zn or Zn–Li alloy and $c$ can be obtained by the (0 0 2) *d*-spaces measured in the present experiment. The estimated solubility of Li for the Zn–Li alloy with 1 and 2 at% Li is close to its nominal Li doping content, implying that dominant Li atoms substitute for Zn sites in the two Zn–Li alloys. Since the solubility of Li in Zn is about 1.5 at%, very close to the estimated value of 1.63 in the Zn–Li alloy with a nominal Li content of 2 at%, the lattice constants will not increase with increasing Li content when the nominal doping content exceeds 2 at%. Therefore, it is deduced that only about 1.67 at% Li incorporates into Zn in a form of substitution for the Zn–Li alloy with 4 at% Li, and the other 2.33 at% Li may exist in the grain boundary of the alloy.

Curves a, b and c in figure 2 show the XRD patterns of the Zn and Zn–Li films with 2 and 4 at% Li annealed in two steps, respectively, indicating the formation of ZnO with a wurtzite structure. Curve a presents only one peak corresponding to the (0 0 2) plane of ZnO, suggesting that the undoped ZnO obtained by annealing Zn has a high (0 0 2) preferential orientation with the *c*-axis perpendicular to the substrate. However, a few weak diffraction peaks of ZnO besides the strong (0 0 2) peak are exhibited in XRD patterns of the annealed Zn–Li alloys, as shown in curves b and c in figure 2, implying that the Li-doped ZnO (denoted as ZnO:Li) has a lower preferred orientation than the undoped ZnO. The lower preferential orientation may be due to a decrease in crystal quality ZnO induced by Li doping. Similar results were observed in the ZnO produced by annealing of Zn and Zn–Li alloy in one step.

It is noted that the *d*-spaces of the (0 0 2) peak for undoped and 2 at% Li-doped ZnO are almost the same, as shown in curves a and b of figure 3, implying the dominant Li atoms in the Li-doped ZnO substituting for the Zn site. Since the

**Table 1.** Electrical properties of ZnO:Li and ZnO prepared by different annealing processes.

| Sample | Nominal Li content (at%) | Annealing ambient | Type | Resistivity (Ω cm) | Mobility ($cm^2\ V^{-1}\ s^{-1}$) | Carrier concentration ($cm^{-3}$) |
|---|---|---|---|---|---|---|
| $A_1$ | 0 | $N_2$, $O_2$ | n | 18.71 | 2.43 | $1.373 \times 10^{17}$ |
| $A_2$ | 0 | $O_2$ | n | 10.19 | 3.12 | $1.963 \times 10^{17}$ |
| $B_1$ | 1 | $N_2$, $O_2$ | n/p | 56.56 | 1.27 | $8.69 \times 10^{16}$ |
| $B_2$ | 1 | $O_2$ | n | 286.27 | 2.32 | $9.398 \times 10^{15}$ |
| $C_1$ | 2 | $N_2$, $O_2$ | p | 678.34 | 1.03 | $8.934 \times 10^{15}$ |
| $C_2$ | 2 | $O_2$ | – | High | – | – |
| $D_1$ | 4 | $N_2$, $O_2$ | n | 95.81 | 0.878 | $7.42 \times 10^{16}$ |
| $D_2$ | 4 | $O_2$ | n | 160.26 | 0.401 | $9.711 \times 10^{16}$ |

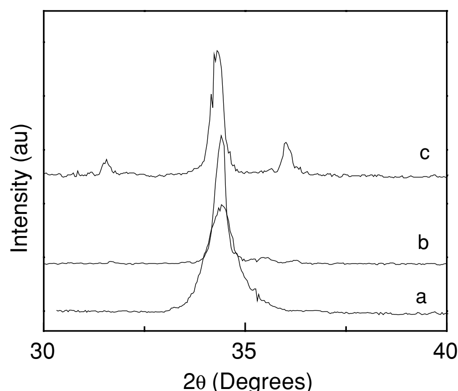


**Figure 3.** XRD patterns of around the (0 0 2) peak of (a) metal Zn, (b) Zn–2 at% Li and (c) Zn–4 at% Li alloy film annealed at 500 °C for 2 h in $N_2$ flow and then at 700 °C for 1 h in $O_2$ flow.

covalent radius of Li (0.123 nm) is almost the same as that of Zn (0.125 nm), change of the ZnO lattice is little when a small amount of Li (such as below 2 at%) substitutes for the Zn lattice site in ZnO, resulting in the undoped and Li-doped ZnO having the same (0 0 2) *d*-spaces. However, as the curve c of figure 3 shows, the (0 0 2) *d*-space of the ZnO doped with nominal 4 at% Li is larger than that of the undoped ZnO. This implies that there exist some $Li_i$ in the ZnO:Li doped with 4 at% Li besides $Li_{Zn}$.

The electrical properties of both undoped and Li-doped ZnO films obtained by Hall measurement are listed in table 1. Due to the insulating properties of quartz, the conducting features of the films are not affected by the quartz substrate and are completely attributed to ZnO films. The data in table 1 were compiled by adopting both positive and negative currents and magnetic fields, and the results were averaged in order to compensate for various electromagnetic effects. The positive Hall coefficient for all six current/field combinations assures that the sample is true p-type. Table 1 shows that both undoped and Li-doped ZnO prepared by annealing in one step are n-type semiconductors except that sample $C_2$ shows a high resistivity, and that only sample $C_1$ shows p-type conduction in all ZnO prepared by annealing in two steps.

It is worth noting that both samples $A_1$ and $C_1$ are prepared by annealing in two steps. But sample $C_1$ shows p-type conduction, while sample $A_1$ shows n-type conduction. The only difference between them is that sample $C_1$ contains Li dopant while sample $A_1$ does not; this implies that the p-type conductive behaviour of sample $C_1$ is mainly associated with Li doping rather than N doping. Li atom may replace the Zn site in the ZnO:Li to form an acceptor during the annealing of the Zn–Li alloy in two steps. It is also found from table 1 that both samples $C_1$ and $C_2$ are ZnO:Li with the same Li doping content, but they have different conduction behaviours. The only difference between them is that sample $C_1$ is prepared by annealing in $N_2$ and $O_2$ flows while sample $C_2$ is produced in $O_2$ flow. This implies that the annealing in $N_2$ ambient has an important role for p-type conduction. Samples $B_1$, $C_1$ and $D_1$ are all Li-doped ZnO and produced by annealing in $N_2$ and $O_2$ ambient, but they have different nominal Li doping concentrations. So, it is concluded that the conduction feature of the Li-doped ZnO is related to the Li concentration.

Much literature has reported that the formation of the Li-doped p-type ZnO film is limited by the formation of $Li_i$ and $Li_{Zn}$–$Li_i$ complex donors [8]. So, the ZnO:Li prepared by annealing in $O_2$ flow, such as samples $B_2$, $C_2$ and $D_2$, shows n-type conduction. However, when the Zn–Li film was annealed in $N_2$ flow at 500 °C, Li in the Zn–Li alloy may react easily with $N_2$ to form a Li–N cluster due to a larger difference in electronegativity between Li and N. When Zn–Li is annealed in $O_2$ ambient to form ZnO:Li, Li–N in the grain can suppress the formation of a donor of $Li_i$ or/and $Li_{Zn}$–$Li_i$ complex. On the other hand, N in Li–N may substitute for the O site in ZnO:Li and bond with three or four Li occupying the Zn site to form the $Li_{Zn}$–N complex acceptor. For sample $B_1$, the $Li_{Zn}$–N complex acceptors may not compensate for donors due to the fact that the Li doping content is small, and is close to the donor in concentration. So, it shows p-type conduction sometimes and n-type sometimes in the Hall measurement process. Based on the results of figure 1 it is deduced that the Li content of sample $C_1$ is nearly twice that of sample $B_1$; therefore, the amount of the $Li_{Zn}$–N acceptor may exceed that of the donors for sample $C_1$, resulting in p-type conduction. However, as mentioned in figure 1, only 1.67 at% Li incorporates into Zn for the Zn–Li alloy with 4 at% Li due to the solubility limit of Li in Zn, and the other 2.33 at% Li exists in the grain boundary. When the Zn–Li alloy was annealed in $N_2$ ambient, Li in the Zn–Li grain may react with N to form a Li–N cluster while Li in the grain boundary will form $Li_3N$. However, in subsequent annealing in $O_2$ ambient, the Li–N cluster forms a $Li_{Zn}$–N complex acceptor as discussed above, while $Li_3N$ in the grain boundary may react with $O_2$ to form $Li_2O$ and $N_2$. Li in $Li_2O$ may incorporate in ZnO:Li in a form of interstitial dopant during the formation of ZnO:Li, which can be confirmed by the result of curve c in figure 3. So, n-type conduction of sample $D_1$ can be associated with the increased interstitial Li dopants in it, which compensate $Li_{Zn}$–N complex acceptors.

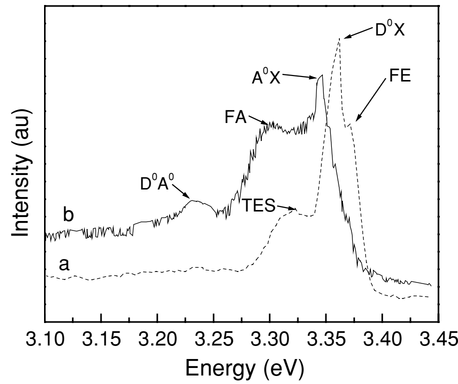


**Figure 4.** PL spectra of (a) n-type undoped ZnO and (b) p-type ZnO:Li measured at 12 K.

Curves a and b in figure 4 show PL spectra of undoped n-type ZnO (sample $A_1$) and p-type ZnO:Li films (sample $C_1$) measured at 12 K, respectively. For the undoped ZnO, the peak at 3.362 eV is dominant and can be associated with donor-bound exciton emission ($D^0X$) [10, 11]. The peak at 3.32 eV was assigned to two-electron satellite (TES) transition of the neutral donor bound exciton based on the results of bulk, nominally undoped ZnO reported by Thonke *et al* [12]. The weak peak at 3.371 eV is ascribed to free exciton emission (FE). The PL spectrum of the p-type ZnO:Li is shown in curve b of figure 4. Obviously, it is different from the PL spectrum of undoped ZnO in both emission peak structure and intensity. As curve b shows, the PL spectrum of p-type ZnO:Li consists of three emission peaks, located at 3.347, 3.302 and 3.234 eV, respectively. The emission peaks intensities are much weaker than those of the undoped ZnO, so it is enlarged by seven times to be presented in figure 4. The 3.302 eV is very close to the emission energy of the conduction band to acceptor level transition (FA) reported in the literature [13, 14], so the 3.302 eV peak is attributed to electron radiate transition from the conduction band to the $Li_{Zn}$–N acceptor level. The 3.234 eV peak is assigned to donor–acceptor pair (DAP) transition, since it is very similar to the emission energy of DAP transition observed in N, P and As-doped ZnO [15, 16]. The peak located at 3.347 eV is the most dominant among the three peaks, as shown in curve b of figure 3. To our knowledge, this peak has not been observed in p-type ZnO reported up to now. According to the literature, the emission energies of acceptor-bound exciton in N-, P- and As-doped ZnO at around 12 K are 3.315, 3.355 and 3.358 eV, respectively [10, 17, 18]. The emission energy of 3.347 eV is in the emission energy range of 3.315–3.358 eV. Due to p-type conduction of ZnO:Li, it is deduced that the 3.347 eV emission peak may be ascribed to a neutral $Li_{Zn}$–N acceptor-bound exciton emission.

The optical $Li_{Zn}$–N complex acceptor level ($E_A$) can be estimated by using the relationship:

$$E_{FA} = E_g - E_A + \kappa_B T/2, \quad (2)$$

where $E_{FA}$ and $E_g$ are the emission energies of the conduction band to acceptor level transition and band gap of ZnO, respectively; $k_B$ is the Boltzmann constant and $T$ is the absolute temperature. At 12 K, the band gap is 3.437 eV [10], $E_{FA}$ is 3.302 eV in the present work, and the thermal energy term in the equation can be neglected. As such, $E_A$ is calculated to be about 137 meV, which is about 47 meV larger than the theoretical value [4].

## Conclusion

Li-doped p-type ZnO film was produced by annealing Zn–2 at% Li alloy film deposited on quartz in two steps. The heat treatment in $N_2$ ambient may lead to the formation of a Li–N cluster in the Zn–Li alloy grain, which suppressed the formation of $Li_i$ and $Li_{Zn}$–$Li_i$ complex donors but resulted in the formation of a $Li_{Zn}$–N complex acceptor in ZnO:Li during annealing in $O_2$ ambient. The optical $Li_{Zn}$–N acceptor level was estimated to be 137 meV. The p-type ZnO:Li has a resistivity of 678.34 Ω cm, a Hall mobility of 1.03 $cm^2$ $V^{-1}$ $s^{-1}$ and a carrier concentration of $8.934 \times 10^{15}$ $cm^{-3}$. Three PL peaks centred at 3.347, 3.302 and 3.234 eV are observed at 12 K and are due to neutral acceptor-bound exciton emission, conduction band to acceptor level transition and donor-acceptor pair recombination emission, respectively.

## Acknowledgments

This work is supported by the programme of CAS Hundred Talents, the Key Projects of National Natural Science Foundation of China under grants 60336020 and 50532050, the Innovation Project of Chinese Academy of Sciences, the National Natural Science Foundation of China under grants 60278031, 60376009, 50402016, 60506014 and 60501025.

## References

[1] Ryu Y R, Zhu S, Look D C, Wrobel J M, Jeong H M and White H W 2000 *J. Cryst. Growth* **216** 330
[2] Yoshino Y, Makino T, Katayama Y and Hata T 2000 *Vacum* **59** 538
[3] Lee J-B, Lee H-J, Seo S-H and Park J-S 2000 *Thin Solid Films* **398–399** 641
[4] Park C H, Zhang S B and Wei S-H 2002 *Phys. Rev.* B **66** 073202
[5] Gonales C, Block D, Cox R T and Herve A 1982 *J. Cryst. Growth* **59** 357
[6] Block D, Herve A and Cox R T 1982 *Phys. Rev.* B **25** 6049
[7] Onodera A, Tamaki N, Kawamura Y and Sakagami N 1996 *Japan. J. Appl. Phys.* **35** 5160 Part 1
[8] Wardle M G, Goss J P and Bridon P R 2005 *Phys. Rev.* B **71** 155205
[9] Look D C 1989 *Electrical Characterization of GaAs Material and Devices* (New York: Wiley)
[10] Look D C, Reynolds D C, Litton C W, Jones R L, Eason D B and Cantell G 2002 *Appl. Phys. Lett.* **81** 1830
[11] Goto T and Langer D W 1971 *J. Appl. Phys.* **42** 5066
[12] Thonke K, Gruber T, Teofilov N, Schonfelder R, Waag A and Sauer R 2001 *Physica* B **308–310** 945
[13] Jeong T S, Han M S, Youn C J and Park Y S 2004 *J. Appl. Phys.* **96** 175
[14] Lee W, Jeong M-C and Myoung J-M 2004 *Appl. Phys. Lett.* **85** 6176
[15] Liang H W, Lu Y M, Shen D Z, Liu Y C, Yan J F, Shan C X, Li B H, Zhang Z Z, Zhang J Y and Fan X W 2005 *Phys. Status Solidi* a **202** 1060
[16] Hwang D K, Kim H S, Lim J H, Oh J Y, Yang J H, Park S J, Kim K K, Look D C and Park Y S 2005 *Appl. Phys. Lett.* **86** 151917
[17] Kim K-K, Kim H-S, Hwang D-K, Lim J-H and Park S-J 2003 *Appl. Phys. Lett.* **83** 63
[18] Ryu Y R and Lee T S 2003 *Appl. Phys. Lett.* **83** 87